RSC Advances

This is an *Accepted Manuscript*, which has been through the Royal Society of Chemistry peer review process and has been accepted for publication.

Accepted Manuscripts are published online shortly after acceptance, before technical editing, formatting and proof reading. Using this free service, authors can make their results available to the community, in citable form, before we publish the edited article. This *Accepted Manuscript* will be replaced by the edited, formatted and paginated article as soon as this is available.

You can find more information about *Accepted Manuscripts* in the Information for Authors.

Please note that technical editing may introduce minor changes to the text and/or graphics, which may alter content. The journal's standard Terms & Conditions and the Ethical guidelines still apply. In no event shall the Royal Society of Chemistry be held responsible for any errors or omissions in this *Accepted Manuscript* or any consequences arising from the use of any information it contains.

ROYAL SOCIETY OF CHEMISTRY

www.rsc.org/advances

Please do not adjust margins

Journal Name

ARTICLE

Investigation of biological cell–small molecular interactions based gold surface plasmon resonance sensor using a laser scanning confocal imaging-surface plasmon resonance system†

Received 00th January 20xx,
Accepted 00th January 20xx

DOI: 10.1039/x0xx00000x

www.rsc.org/

Sha Liu[a,b], Hongyan Zhang[a,*], Weimin Liu[a], Bingjiang Zhou[a], Qian Ma[a,c], Jiechao Ge[a], Jiasheng Wu[a], Pengfei Wang[a]

In our work, we investigated the interaction between small molecule–folic acid and biological cell through the interaction of folic acid and folate receptor with the use of laser scanning confocal imaging-surface plasmon resonance (LSCI-SPR) system. Changes between SPR peaks and cell concentrations had good linear relationships, and fluorescent imaging provided further identified datum. Detection limit was as low as 1.0×10^3 cells/mL, and linear coefficients were 0.95206, 0.95454, 0.94287, 0.98711, and 0.99228 for mouse lymphoma (L5178Y TK+/-) cells, mouse lymphoma (EL4) cells, mouse T lymphocytes (Cl.Ly 1+2-/9) cells, human lung cancer (A549) cells, and human oral epidermis carcinoma (KB) cells, respectively. Results indicated that the LSCI-SPR system has potential future application in analyzing small molecule–biologic cell affinity and in acquiring quantitative parameters.

Introduction

Folic acid (FA) is an important vitamin for cell growth, differentiation, and homeostasis.[1–6] For existing pre-neoplastic and neoplastic lesions in animals, FA supplementation increases tumor burden, and different amounts of folic acid receptor (FAR) proteins exist on the cell surface.[7,8] FAR has low expression in normal tissues but has high expression in malignant epithelial cells, including ovary, brain, kidney, breast, colon, lung, and myeloid, which have high affinity with FA (Kd<1 nM).[9] Hence, exploiting these unique characteristics of differential FAR overexpression through strong interaction of FA-FAR on surfaces of living cells is important in the fields of cancer diagnosis, therapy, and imaging.[10–14] Many studies have been conducted on the interaction mechanism between FA and FAR. Results show that FAR has a globular structure stabilized by eight disulfide bonds and contains a deep, open folate-binding pocket that comprises residues conserved in all receptor subtypes; therefore, FAR has high affinity with FA.[15,16] Many researchers have investigated the effects of anti-cancer drugs by labeled and free-labeled method.[17,18] Normally, an in-depth understanding of the interaction between biologic cell and biomolecule is the key to identifying a favorable method in relative physiological processes to cure and control diseases, including cancers, diabetes, and some genetic ailments in biological processes of organisms.[19,20] With the advancement in proteomics, a wide range of methods have been developed for investigating biomolecular interactions, such as enzyme-linked immunosorbent assay, fluorescence resonance energy transfer, laser scanning confocal imaging (LSCI) microscopy, chromatography, and co-immunoprecipitation.[21–24] These methods not only require label markers but also destroy biomolecular structures and properties easily, which limit their applications in practice.[25–27] Surface plasmon resonance (SPR) and surface plasmon resonance imaging have been the most widely-used techniques for in situ and real-time measurements of surface probe–target interactions based on gold metal nano-structure surface.[28–31] Commercial instruments based on SPR theory have been developed and extensively used to trace contaminants in water, food, and air because of the highly sensitive optical reflectivity of gold film to dielectric changes in environment.[32–35] Biologic cell action has been monitored by SPR method.[36,37] However, small molecule–biologic cell interaction is difficult to investigate using free-labeled method because of their low molecular weight, although interactions of a few small molecules have been achieved through special modification with large molecules or nanoparticles.[38,39] Detecting small molecule–biologic cell interaction directly and effectively is still a challenge. In our previous work, we developed an LSCI-SPR system to monitor big molecule–biological cell interaction. We achieved quantitative results by identifying real-time nonspecific adsorption to detect biologic cell–protein interaction.[25,40]

[a] Key laboratory of Photochemical Conversion and Optoelectronic Materials, Technical Institute of Physics and Chemistry, Chinese Academy of Sciences, Beijing, 100190, China;E-mail: zhanghongyan@mail.ipc.ac.cn; Tel: +86-10-82543475; Fax: +86-10-82543512;
[b] University of Chinese Academy of Sciences, Beijing, 100049, China
[c] Beijing Key Laboratory of Optical Detection Technology for Oil and Gas, China University of Petroleum, Beijing 102249, China
†Electronic Supplementary Information (ESI) available: See DIO 10.1039/x0xx00000x

RSC Advances Accepted Manuscript

In this paper, the LSCI-SPR system is used to monitor small molecule FA–biologic cell interactions, which are DiO labeled and includes suspended and adherent cancer cells with different FAR expression levels. Owing to specific interactions between FA and FAR on the cancer cell membrane, cancer cells can be assembled on an FA-modified SPR sensor chip. With the change in cell concentration, SPR signals and fluorescent images are synchronously recorded in real time. FA reactions with different FAR cells through the binding process are observed and ascertained from the SPR signal. Binding rate values are also acquired through FA–FAR interactions on membranes of different adherent and suspended biologic cells by using a simple and rapid-preparation process. Green fluorescent points on SPR sensor chip increased with the increasing cancer cell concentrations and fitted well with the changes in SPR signals. This method has potential application in direct detection of cancer cells by small molecule–biological cell special interaction. I

Experiment

Materials and reagents

FA, dimethyl sulfoxide (DMSO), and cysteamine were purchased from Sigma (St. Louis, MO, USA). 1-(3-dimethylaminopropyl)-3-ethylcarbodiimide hydrochloride (EDC) and N-hydroxysuccinimide (NHS) were obtained from Huamei Biotechnology Co., China. 3,3'-Dioctadecyloxacarbocyanine perchlorate (DiO) was purchased from Molecular Probe, Inc. All biological reagents were kept in a refrigerator at 4 °C. All other chemicals were of analytical reagent grade. All solutions were prepared with ultrapure water (18.4 MΩ·cm, Millipore Corp.). Exactly 0.3 mol/L citrate buffer (pH 2.7) and 0.1 mol/L phosphate-buffered saline (PBS, pH 7.4) were prepared. Mouse lymphoma (L5178Y TK+/-) cells, mouse lymphoma (EL4) cells, mouse T lymphocytes (Cl.Ly 1+2-/9), human lung cancer (A549) cells, and human oral epidermis carcinoma (KB) cells were provided by the Center of Cells, Peking Union Medical College.

LSCI-SPR instrument

The LSCI–SPR experimental setup and the biosensor substrates were described in Fig. S1 which were integrated with an angle modulated SPR with a laser scanning confocal microscope. A 10× objective (Nikon CFI Plan Apochromat, N.A. 0.30, W.D. 16 mm, Spring-loaded) was used for imaging, and Dio was excited by a sapphire solid laser at 488 nm with 50.1% intensity ratio and M pin hole. The biosensor substrates were prepared by sputtering 2 nm Cr and 48 nm Au onto LaSFN9 (n=1.83) slides with much (111) plane and less (222) plane (Fig. S2). The side of the slide with Au film was immersed in the flow cell with a 0.13 mm-thick bottom, and the blank side was attached to the prism using refractive index matching liquid. The prism, substrate, and flow cell were fixed on the stage of the inverted microscope of the LSCM (Nikon C1 Si, Japan) system. The focal plane was positioned on the gold film to detect the fluorescence image when the cancer cells were inserted in the flow cell. Two rotary stages (KS432-75, Japan) are vertically mounted coaxially with all the incident optics components and the detection devices are fixed on two Alum boards separately. The angle of incidence was freely varied by adjusting the rotation arms on the instrument by two rotary stages, and the resonance minimum at a given angle was positioned accordingly. The samples are injected into flow cell by a spring pump (Harvard 33 Twin Syringe Pump, USA). He-Ne laser focused into a polarization maintaining fiber, and the fiber was fixed on one of the Alum board. The incident light went into a collimator. After a polarization, the light became P- polarities. A chopper (SR540, USA) was put before the LaSFN9 prism, and the reflect light signal from photodiode (Dsi300, China) was analyzed by a lock-in amplifier (SR830, USA).The samples were then injected into the flow cell through a spring pump (Harvard 33 Twin Syringe Pump, USA). The LSCI–SPR instrument can successfully monitor the process of special interaction in real time and in situ by combining the virtues (identifying the interaction between the biomolecule and biologic cell and imaging) of SPR and LSCI.

Cell culture and preparation of cell solutions

L5178Y and EL4 were grown in RPM1640 supplemented with 10% fetal bovine serum and 1% penicillin/streptomycin, and incubated under 5% CO_2 at 37 °C. Cl.Ly was grown in RPM1640 supplemented with 10% fetal bovine serum, 100 u/mL IL-2, and 1% penicillin/streptomycin, and incubated under 5% CO_2 at 37 °C. Adherent cells A549 and KB were grown in McCoy's 5A and RPM1640, respectively, supplemented with 10% fetal bovine serum and 1% penicillin/streptomycin, and incubated under 5% CO_2 at 37 °C. A549 and KB cells were dissociated by trypsin for suspension.

Then, cell suspension concentrations (4 mL) were adjusted to 1.0×10^3, 3.3×10^3, 1.0×10^4, 3.3×10^4, 1.0×10^5, 3.3×10^5, and 1.0×10^6 cells/mL. An appropriate volume of cell culture was concentrated by centrifugation at 1000×g for 3 min for all the cells. Supernatant was removed; cells were resuspended in a 4 mL culture medium that contained 1 μg/mL Dio. Then, samples were incubated under 5% CO_2 at 37 °C for 20 min. All cells were cultured in a carbon dioxide incubator until the concentration reached more than 1.0×10^6 cells/mL. After the medium was removed, cells were rinsed once by PBS and then resuspended in PBS. Cell solutions were diluted to 1.0×10^3, 3.3×10^3, 1.0×10^4, 3.3×10^4, 1.0×10^5, 3.3×10^5, and 1.0×10^6 cells/mL by plate counting.

LSCI-SPR sensor-chip fabrication and characterization

Biosensor substrates were rinsed with ultrapure water, treated with ethanol for 5 min, and then rinsed with ultrapure water again. Fig. 1 shows the cell modification process and sensing principle. Treated substrates were soaked in 10 mmol/L cysteamine solution for 24 h to form a self-assembled monolayer on the gold surface, because the sulfide bond of cysteamine can adhere firmly to gold. The 200 mg FA was added in 15 mL DMSO and dissolved completely by ultrasonic heating treatment for 20 min. Then, 20 mg NHS and 32 mg EDC were added to the FA solution. The mixed solution was diluted to 20 mL with ultrapure water. FA carboxyl group was activated by NHS and EDC for 30 min. Then, activating FA mix solution was pumped from the sensor chip surface, which was covered with cysteamine at a 1 μL/min reaction rate to be assembled on the surface.

RSC Advances Accepted Manuscript

This journal is © The Royal Society of Chemistry 2016

Please do not adjust margins

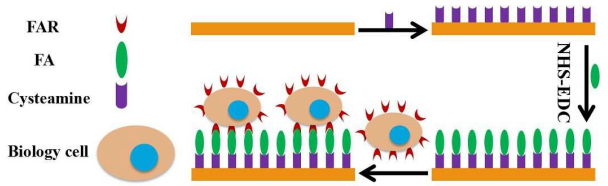

Fig. 1. Schematic of SPR chip modification and interaction with biological cells.

Fourier transform infrared (FTIR) spectra confirmed the presence of cysteamine and folic acid on the gold surface. A comparison of the FTIR spectra of bare gold film, cysteamine assembled on the gold film, and FA that reacted with cysteamine on the gold surface is shown in Fig. S3. The FTIR spectra of cysteamine-covered gold film exhibited absorption peaks at 3556 and 2933 cm^{-1} (black curve in Fig. S3), which corresponded to N-H functional groups and C-H bonding mode of cysteamine according to the previous study.[41] The most characterized peaks of FA at 1690 (amide I) and 1572 (amide II) became more prominent and intense in Au–cysteamine–FA conjugate (red curve in Fig. S3). This result may provide evidence for extra amide bond formation during FA attachment, as described in previous work.[42] FA assembly was carried out for 3 h to organize the processing on the solid surface and form a stable biosensor membrane. Then, PBS buffer was used to wash off the non-covalently bound FA until the SPR signal reached the steady state (Fig. S3), thereby indicating that excess EDC, NHS, and FA were removed from the sensor surface. DiO-labeled cells of different kinds and concentrations were injected into the flow cell at a rate of 200 μL/min and bonded to FA because of the strong FA–FAR interaction at 37 °C. Cysteamine coverage on the gold film was estimated to be approximately 200 ng/cm^2 (2.592×10^{-9} mol/cm2), as shown in Fig. S4, by using the method mentioned by Wang (100 mDgree changes were induced by 100 ng/cm^2 coverage on SPR sensor surface).[43]

SPR measurements

SPR signal data were collected with LabVIEW program. SPR peaks were denoted in degrees. Different SPR signals according to changes in cell concentrations and types were achieved by setting the degree of PBS without cells as a reference and fixed on a point of resonance peak with max slope. All experiments were conducted under the same conditions.

Results and discussion

Real-time monitoring of cell-biosensor chip preparation

To identify FA from a self-assembled monolayer on the surface of the gold, the real-time modification processes were recorded at every modifying step (Fig. S4). First, when cysteamine flowed over the gold chip, the SPR peak began to move, and the peak moved from 58.58° to 58.82° during the modification process. Moreover, the peak increased by 0.20° after FA flowed over the gold chip. After L5178Y cells flowed over the gold chip, SPR peak reached to 59.33°, and the angle changed by 0.75° compared with the bare gold chip. Hence, the strongest response occurred when cells flowed over the chip surface, which is attributed to self-assembled cells on the gold surface by FA–FAR interaction.[44–45] Results indicate that FA was successfully modified on the gold surface. Cells were specifically bound on the gold surface through the strong interaction of FA and FAR (green line in Fig. S5). Without FA, cells cannot self-assemble on the gold surface (black and red lines in Fig. S5).

FA and L5178Y cell interaction

FA has a high-binding affinity for tumor cells because of the large amount of FAR on the tumor cell membrane. First, we chose L5178Y cell to study the interaction between the small molecule FA and the cell. When the cell sensor chip was prepared, DiO-labeled L5178Y cells with different concentrations flowed over the FA-modified gold chip. Real-time interaction processes were recorded by SPR (Fig. 2). With increasing cell concentration, the SPR-absorbing peak moved to the large angle (Fig. 2a). As shown in Fig. 2b, the SPR response peak changed from 59.00° to 59.52° in the stable situation with L5178Y cell concentration changing from 1.0×10^3 cells/mL to 1.0×10^6 cells/mL. L5178Y cell concentration of as low as 1.0×10^3 cells/mL could even be detected easily within half an hour. The calibration curve of cell concentration and SPR peak angle is shown in Fig. 3. Cell concentration and SPR peak angle had a good linear relationship, as indicated by a linear coefficient of 0.95206.

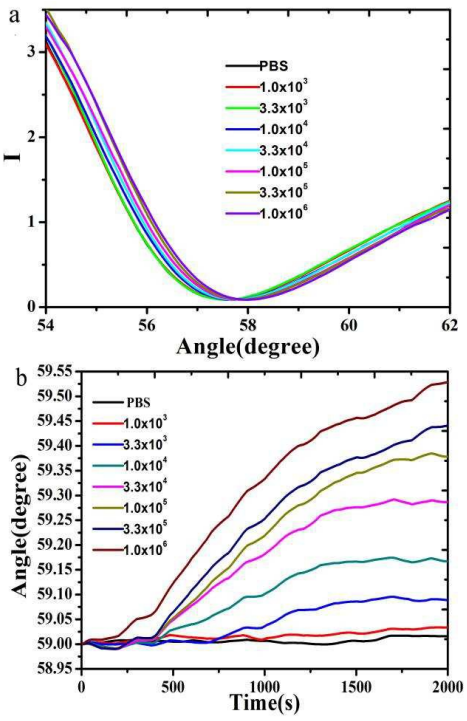

Fig. 2. L5178Y capture process by the SPR sensor chip: (a) moving angle of the SPR peak with changes in different concentrations (1.0×10^3, 3.3×10^3, 1.0×10^4, 3.3×10^4, 1.0×10^5, 3.3×10^5, and 1.0×10^6 cells/mL in PBS buffer); (b) real-time dynamic interaction curve between FA and L5178Y cell in different concentrations from 1.0×10^3 cells/mL to 1.0×10^6 cells/mL.

RSC Advances Accepted Manuscript

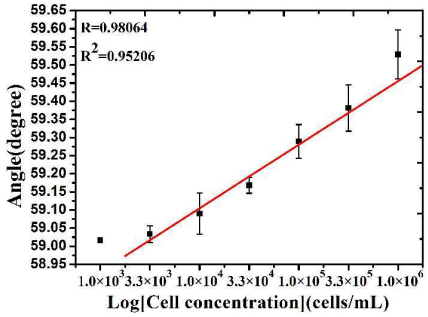

Fig. 3. SPR response with different L5178Y cell concentrations from 1.0×10^3 cells/mL to 1.0×10^6 cells/mL in the PBS solution. Error bars represent the standard deviations taken from at least three independent measurements.

To identify FA–cell specific interaction, L5178Y cell suspensions flowed over the bare gold chip, cysteamine- modified gold chip, and FA-modified gold chip at a rate of 200 μL/min. After flowing for 1,000 seconds, PBS solution was injected into the flow cell by using a 400 μL/min flow rate. SPR signal returned to the same level as the initial level for the two previous chips. Only the third chip maintained a high-level SPR signal, which means that the cells could interact with FA specifically (Fig. S5). We also collected fluorescent images at 1.0×10^3, 1.0×10^4, 1.0×10^5, and 1.0×10^6 cells/mL concentrations in the PBS solution. A clear green fluorescent image with high brightness and contrast was observed because DiO-labeled cells are bound to the sensor chip (Fig. 4). With the increased cell concentration, the number of green points in the view region also increased, thereby indicating that L5178Y cells attached to the surface of SPR chip by FA–FAR interaction on the L5178Y cell membrane. When the cell concentration reached 1.0×10^6 cells/mL, the cells congregated and formed much brighter fluorescent blocks on the sensor chip surface to induce a strong SPR response.

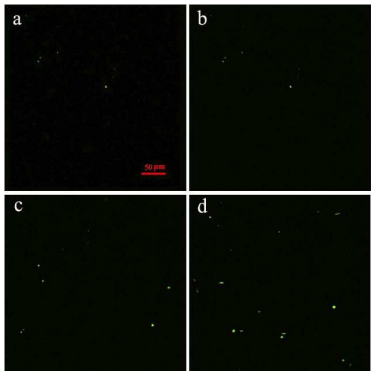

Fig. 4. Fluorescent images obtained from the covering of the L5178Y cells by interacting with folic acid that self-assembled on the gold film at different concentrations in the PBS solution. Letters a, b, c, and d show the L5178Y cell conditions at 1.0×10^3, 1.0×10^4, 1.0×10^5, and 1.0×10^6 cells/mL interacting with modified FA on the chip surface. (The scale bar of all fluorescent images is 50 μm.)

Binding process of FA and other cells

To determine the response of the SPR sensor chip to other cells, A549, Cl.Ly, KB, and EL4 cell suspensions were prepared with different concentrations to flow over the SPR sensor chip. SPR spectra were recorded in real time by the LSCI-SPR system (Fig. S6). Under the same condition with L5178Y, cell concentration and SPR peak had good linear relationships. Linear coefficients for A549, Cl.Ly, KB, and EL4 cells were 0.99228, 0.98711, 0.95494 and 0.94287, respectively (Fig. 5). After the SPR signals were recorded, fluorescent images were collected under the same condition (Fig. 6). With the increase of the concentration from 1.0×10^3 cells/mL to 1.0×10^6 cells/mL, an increasing number of green dots appeared in the fluorescent images for A549, KB, Cl.Ly, and EL4 cell.

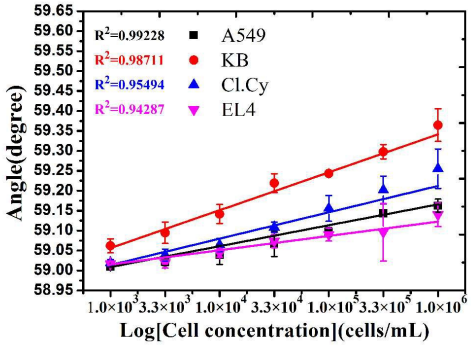

Fig. 5. SPR response with different concentrations from 1.0×10^3 cells/mL to 1.0×10^6 cells/mL for A549, KB, Cl.Ly, and EL4 in PBS buffer. Error bars represent the standard deviations taken from at least three independent measurements.

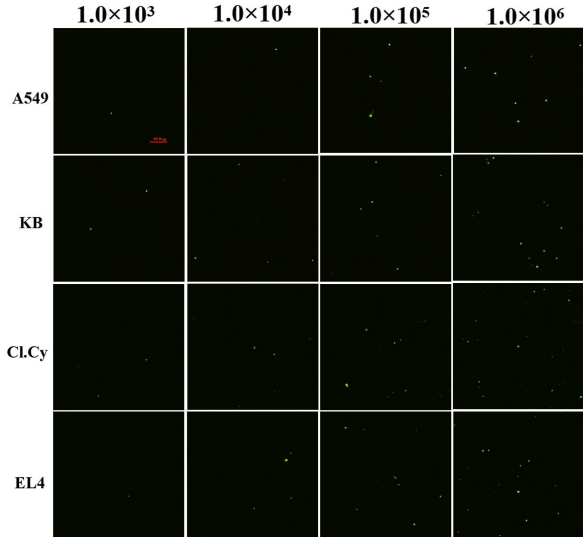

Fig. 6. Fluorescent images obtained from the covering of the sensor chip with different cells at different concentrations in PBS buffer. The first line to the last line represent the changing concentrations of A549, KB, Cl.Ly, and E14 cells from 1.0×10^3 to 1.0×10^6 cells/mL, respectively. (The scale bar of all fluorescent images is 50 μm.)

RSC Advances Accepted Manuscript

This journal is © The Royal Society of Chemistry 2016

Please do not adjust margins

To determine the affinity between FA and different cells, binding rates were estimated according to a real dynamic process at 1.0×10^6 cells/mL for L5178Y, A549, KB, Cl.Ly, and EL4 cells (Fig. S6) using d(degree)/dt; the results are 3.02×10^{-4}/s, 8.05×10^{-5}/s, 1.99×10^{-4}/s, 3.69×10^{-6}/s, and 8.09×10^{-5}/s, respectively. For adherent cells, the KB cell had a larger SPR response peak and binding rate value than those of the A549 cell at the same concentration, which means that KB membrane has a higher FAR expression than A549 cell; this finding is consistent with the findings of Parker.[6] For suspended cells, L5178Y cell membrane has the highest FAR expression, thereby enabling the LSCI-SPR system to identify the FAR expression of suspended cells. Some types of suspended cell may have higher FAR expression than adherent cells. Further experiments should be conducted in the future by using biological method to verify these results.[6,7]

Conclusions

We demonstrated a new method for monitoring the affinity of small molecule and suspended and adherent cells in PBS solution by using an angle-modulated LSCI-SPR system. Cells bound to the surface of SPR through the interaction between FA and their receptor on cell membrane. The sensor chip exhibited an obvious response to cells and could even detect 1.0×10^3 cells/mL concentration in real time. Under the same condition, these cells exhibited different interactions with the self-assembled FA sensor chip, and the binding rate values were estimated according to the dynastic line. This study is the first to identify suspended cell–small molecule interaction. The proposed method has potential application in cancer cell recognition for further development of specific receptors.

Acknowledgments

This work has been supported by the National Nature Science Foundation of China (Grant No. 61378044, 61227008 and 60978034) and the Instrument Developing Project of the Chinese Academy of Sciences (Grant No. YZ201235).

References

1 J. N. Peake, A. J. Copp, J. Shawe, *Birth Defects Research (Part A)*, 2013, **97**, 444–451.
2 R. I. Pinhassi, Y. G. Assaraf, S. Farber, M. Stark, D. Ickowicz, S. Drori, A. J. Domb, Y. D. Livney, *Biomacromolecules*, 2010, **11**, 294–303.
3 Y. Chen, W. Cao, J. Zhou, B. Pidhatika, B. Xiong, L. Huang, Q. Tian, Y. Shu, W. Wen, I-M. Hsing, H. Wu, *ACS Appl. Mater. Interfaces*, 2015, **7**, 2919−2930.
4 S. Boca-Farcau, M. Potara, T. Simon, A. Juhem, P. Baldeck, S. Astilean, *Mol. Pharmaceutics*, 2014, **11**, 391−399.
5 S. Dong, H. J. Cho, Y. W. Lee, M. Roman, *Biomacromolecules*, 2014, **15**, 1560−1567.
6 N. Parker, M. J. Tum, Westrick, E. Lewis, J. D. Low, P. S. Leamon, C. P. Leamon, *Anal. Biochem.*, 2005, **338**, 284−293.
7 M. A. van Dongen, J. E. Silpe, C. A. Dougherty, A. K. Kanduluru, S. K. Choi, B. G. Orr, P. S. Low, M. M. Banaszak Holl, *Mol. Pharmaceutics*, 2014, **11**, 1696–1706.
8 L. Pellis, Y. Dommels, D. Venema, A. van Polanen1, E. Lips, H. Baykus,F. Kok, E. Kampman, J. Keijer, *British Journal of Nutrition*, 2008, **99**, 703–708.
9 A. C. Antony, *Blood*, **79**, 2807-2820.
10 Z. Wang, J. Zhu, Y. Chen, K. Geng, N. Qian, L. Cheng, Z. Lu, Y. Pan, L. Guo, Y. Li and H. Gu, *RSC Adv.*, 2014, **4**, 7483-7490.
11 S. V. Lale, A. Kumar, S. Prasad, A. C. Bharti, and V. Koul, *Biomacromolecules*, 2015, **16**, 1736–1752.
12 X. Zhao and P. Liu, *RSC Adv.*, 2014, **4,** 24232-24239.
13 M.Tagaya, T. Ikoma, Z. Xu, and J. Tanaka, *Inorg. Chem.*, 2014, **53**, 6817–6827.
14 L. Fu, L. Liu, Z. Ruan, H. Zhang and L. Yan , *RSC Adv.*, 2016, Accepted Manuscript DOI: 10.1039/C6RA05657A.
15 C. Chen, J. Ke, X. E. Zhou, W. Yi, J. S. Brunzelle, J. Li, E.-L. Yong, H. E. Xu, K. Melcher, *Nature*, **500**, 486-489.
16 R. I. Pinhassi, Y. G. Assaraf, S. Farber, M. Stark, D. Ickowicz, S. Drori, Y. D. Livney, *Biomacromolecules*, 2009, **11**, 294-303.
17 M. Santucci, T. Vignudelli, S. Ferrari, M. Mor, Laura S., M. L. Bolognesi, E. Uliassi, M. P. Costi, *J. Med. Chem.*, 2015, **58**, 4857–4873.
18 B. Subia, T. Dey, S. Sharma, S. C. Kundu, *ACS Appl. Mater. Interfaces*, 2015, **7,** 2269–2279.
19 C. Yan, T. Kaoud, S. Lee, K. N. Dalby, P. Ren, *J. Phys. Chem. B*, 2011, **115**, 1491-502.
20 A. K. Arakaki, R. Mezencev, N. J Bowen, Y. Huang, J. F. McDonald, J. Skolnick, *Molecular Cancer*, 2008, **7**, 1476-4598.
21 L. L. Jaeger, A. Daniel Jones, B. D. Hammock, *Chem. Res. Toxicol.*, 1998, **11**, 342–352.
22 J. J. Rindermann, Y. Akhtman, J. Richardson, T. Brown, P. G. Lagoudakis, *J. Am. Chem. Soc.*, 2011, **133**, 279–285.
23 T. P. Burghardt, K. Ajtai, J. Borejdo, *Biochemistry*, 2006, **45**, 4058–4068.
24 G. Arrigoni, M. A. Pagano, S. Sarno, L. Cesaro, P. James and L. A. Pinna, *J. Proteome Res.*, 2008, **7**, 990–1000.
25 H. Zhang, L. Yang, B. Zhou, W. Liu, J. Ge, J. Wu, Y. Wang, P. Wang, *Biosens. Bioelectron.*, 2013, **47**, 391–395.
26 S. Liu, H. Zhang, J. Dai, S. Hu, I. Pino, D. Eichinger, H. Lyu, H. Zhu, mAbs, *Taylor & Francis*, 2015, **7**, 110–119.
27 H. Zhang, R. Liang, W. Li, K. Jin, Y. Zhou, K. Ruan, G. Yang, *Chinese Physics B*, 2008, **17**, 2288–2304.
28 X. Wang, J. Xu, C. Liu and Y. Chen, *RSC Adv.*, 2016, **6**, 21900-21906.
29 A. J. Wood, B. Chen, S. Pathan, S. Bok, C. J. Mathai, K. Gangopadhyay, S. A. Grant and S. Gangopadhyay, *RSC Adv.*, 2015, **5**, 78534-78544.
30 D. Bhattacharyya, P. K. Sarswat, M. Islam, G. Kumar, M. Misra and M. L. Free, *RSC Adv.*, 2015, **5**, 70361-70370.
31 X. Yang, Y. Wang, K. Wang, Q. Wang, P. Wang, M. Lin, N. Chen and Y. Tan, *RSC Adv.*, 2014, **4**, 30934-30937.
32 J. Wang, A. Munir, Z. Zhu, H. Susan Zhou, *Anal. Chem.*, 2010, **82**, 6782–6789.
33 W-C. Law, K-T. Yong, A. Baev, P. N. Prasad, *ACS Nano*, 2011, **5**, 4858–4864.
34 M. Lütfi Yola, N. Atar, A. Erdem, *Sensors and Actuators B: Chemical*, 2015, **221**, 842–848.
35 X. Liu, Y. Yang, L. Mao,Z. Li, C. Zhou, X. Liu, S. Zheng, Y. Hu, *Sensors and Actuators B: Chemical*, 2015, **218**, 1-7.
36 F. Zhang, S. Wang, L. Yin, Y. Yang, Y. Guan, W. Wang, H. Xu, and N. Tao, *Anal. Chem.*, 2015, **87**, 9960–9965.
37 C. Liu, S. Alwarappan, H. A. Badr, R. Zhang, H. Liu,J-J. Zhu, and C-Z. Li, Anal. Chem., 2014, 86,7305–7310
38 P. Canoa, R. Simón-Vázquez, J. Popplewell, Á. González-Fernández, *Biosens. Bioelectron.*, 2015, **74**, 376-383.

RSC Advances Accepted Manuscript

39 S. H. Baek, A. W. Wark, H. J. Lee, *Anal. Chem.*, 2014, **86**, 9824–9829.
40 H. Zhang, L. Yang, B. Zhou, X. Wang, G. Liu, W. Liu, P. Wang, *Spectrochimica Acta Part A: Molecular and Biomolecular Spectroscopy*, 2014, **21**, 381–386.
41 A. Rai, C. C. Perry, *Langmuir*, 2010, **26**, 4152–4159.
42 C. P. Leamon, J. A. Reddy, I. R. Vlahov, M. Vetzel, N. Parker, J. S. Nicoson, L-C Cu, E. Westrick, *Bioconjugate Chemistry*, 2005, **16**, 803-811.
43 L. Wang, T. Li, Y. Du, C. Chen, B. Li, M. Zhou, S. Dong , *Biosens. Bioelectron.,* 2010, **25**, 2622–2626.
44 J. Qiao, P. Dong, X.Mu, L.Qi, R.Xiao, *Biosens. Bioelectron.*, 2016, **78**, 147-153.
45 R. M. Devendiran, S. k. Chinnaiyan, N. K. Yadav, G. Ramanathan, S. Singaravelu, P. T. Perumal, U. T. Sivagnanam, *RSC Adv.*, 2016, **6**, 32560-32571.
46 P. M. S. D. Cal, R. F. M. Frade, V. Chudasama, C. Cordeiro, S. Caddick, P. M. P. Gois, *Chem. Commun.*, 2014, **50**, 5261-5263.

RSC Advances Accepted Manuscript

This journal is © The Royal Society of Chemistry 2016